16TH EUROPEAN CONFERENCE ON EARTHQUAKE ENGINEERING THESSALONIKI 18 - 21 JUNE 2018

SEISMIC RETROFIT OF STEEL TALL BUILDINGS WITH BILINEAR OIL DAMPERS

Sarven AKCELYAN[1], Dimitrios G. LIGNOS[2]

ABSTRACT

This paper presents retrofit solutions for existing tall buildings by utilizing supplemental damping devices, namely oil dampers with relief valve (bilinear oil dampers). To this end, multiple retrofit schemes are presented for a benchmark 40-story steel moment-resisting frame building designed in 1970s in North America. This building has a high collapse risk based on the regional seismic hazard and rigorous nonlinear response history analyses that were conducted with state-of-the-art nonlinear building model representations. Nine retrofit schemes are designed based on three damping levels and three vertical damping distribution methods (i.e. effective, direct and balanced shear force proportional damping distributions). The oil dampers are designed with the aid of a multi-degree of freedom (MDF) performance curves tool. A balanced distribution method is proposed to provide an alternative vertical damping distribution method for frames that exhibit yielding. To assess the proposed retrofit schemes, rigorous nonlinear response history analysis of the retrofitted schemes are carried out in accordance to ASCE 41-13 recommendations. The results suggest that supplemental damping can significantly reduce the collapse risk and control the drift distribution along the building height. The effectiveness of the vertical damping distribution methods is strongly influenced by the extent of frame inelasticity, which in turn depends on the supplemental damping level. Although damper velocity demands may exceed the expected values in a low probability of occurrence seismic event, the corresponding damper forces remain relatively constant. In addition, a large amount of linear supplemental damping is provided at low and moderate ground shaking intensities.

Keywords: Collapse risk; supplemental damping; seismic retrofit; bilinear oil dampers; tall buildings

1. INTRODUCTION

Moment-resisting steel space frames were one of most utilized lateral force resisting systems in the design practice of tall buildings in West Coast of North America between 1960 and 1990s (Almufti et al. 2012). Many of these buildings were not designed to meet capacity design requirements. The seismic design loads were not based on rigorous seismic hazard assessment and tools to conduct modern advanced analysis methods were fairly limited. Recent studies underscored the need for seismic retrofit of these buildings (Bech et al. 2015; Lai et al. 2015; Hutt et al. 2016). Conventional retrofit techniques often increase the seismic demands on frame members. Therefore, using supplemental damping devices, particularly, velocity-dependent dampers can be a strategy to minimize the frame internal force demands. For instance, fluid viscous devices have been utilized for this purpose (Constantinou et al. 1993; Symans and Constantinou 1998; Uriz and Whittaker 2001; Symans et al. 2008; Malley et al. 2011; Lai et al. 2015). As an alternative to nonlinear viscous dampers, bilinear oil dampers are widely used in tall buildings in Japan. The efficiency of these dampers has been demonstrated in recent experimental and numerical studies (Kasai et al. 2013a; Kasai and Matsuda 2014). Notably, tall buildings equipped with oil dampers showed promising performance during the 2011 Tohoku earthquake in Japan (Kasai et al. 2013b).
To the best of our knowledge the implementation of bilinear oil dampers has not been studied for pre-

[1]PhD, Course Lecturer, McGill University, Montreal, Canada, sarven.akcelyan@mail.mcgill.ca
[2]Associate Professor, EPFL, Lausanne, Switzerland, dimitrios.lignos@epfl.ch

Northridge North American buildings to date. This paper demonstrates seismic retrofit strategies with bilinear oil dampers for a benchmark 40-story steel moment-resisting frame (MRF) building. Multiple retrofit schemes are explored to demonstrate the effect of various damping levels and distribution methods on the nonlinear behavior of the building.

2. SEISMIC ASSESSMENT OF THE CASE STUDY BUILDING

2.1 Description of the Prototype Building

The benchmark building to be retrofitted is representative of tall steel buildings designed in 1970s in the West Coast of the US. It is located in San Francisco. A building with similar characteristics was studied by Hutt et al. (2016). Figure 1 shows the plan and elevation views of the 40-story building including 3 stories below the ground floor. The building is 154.7 m (507.5 ft) tall above the ground level and has plan dimensions of 24.4 m by 36.6 m (80 ft by 120 ft) with a typical story height of 3 m (10 ft). It is designed as an office building per UBC 1973 (ICBO 1973). The lateral load resisting system consists of space MRFs. The beams are made of W-shape using A36 [248 MPa (36 ksi)] steel, while columns utilize box sections using ASTM A572 Gr. 42 [290 MPa (42 ksi)] steel. According to UBC 1973 (ICBO 1973), the seismic design base shear is 0.021W, while the design wind base shear forces are 0.027W and 0.018W in the X- and Y-loading directions, respectively. The steel design is mainly governed by the wind load drift limitation (0.25%), particularly in the lower stories. The peak column axial load due to the effective gravity load $P_{c,G}$ is 0.32$P_{y,ec}$, where $P_{y,ec}$ is the expected axial yield strength of the column. The design highly violates the strong column-weak beam requirements.

2.2 Seismic Assessment per ASCE-41-13

Two dimensional (2D) models of the building are developed in *OpenSees* (McKenna 1997) platform for both loading directions. The models consider the nonlinear behavior of structural components including columns, beams and panel zones. Beams are modeled using an elastic beam-column element with concentrated plasticity spring elements at the column faces (Ibarra and Krawinkler 2005; Zareian and Krawinkler 2006). Both ductile and brittle behaviors of beams are considered. The beams in pre-Northridge beam-to-column connections are represented by utilizing moment-rotation relations recommended by Lignos et al. (2018), while ductile beams are modeled based on recommendations proposed by Lignos and Krawinkler (2011). Box columns are modeled with a single force-based distributed plasticity beam-column element utilizing five integration points. At stories with column splices two elements are considered. Column splices are not modeled explicitly, assuming that they will be upgraded as part of the retrofit solution. Nevertheless, stresses at splice sections are recorded to identify possible splice failures and the necessity of splice upgrade (Galasso et al. 2015; Stillmaker et al. 2016). The panel zone shear deformation was based on a trilinear shear force-shear distortion model proposed by Krawinkler (1978).

The fundamental periods of the building are around 5.30 sec in both loading directions. Nonlinear static analysis is conducted based on a first-model lateral load pattern. The first yielding is observed at a base shear of 0.06W and 0.5% roof drift and the peak base shear was 0.09W in both loading directions. At around 1% roof drift multiple-story mechanisms develop in the lower part of the building in both loading directions.

The building assessment is based on two earthquake hazard levels, BSE-1E (Basic Safety Earthquake) and BSE-2E hazard levels as suggested in ASCE 41-13 (ASCE/SEI 2014). The former and the latter have a probability of exceedance of 20% and 5% in 50 years, respectively. To this end, 40 ground motions are selected based on site-specific seismic hazard and scaled to be compatible with the uniform hazard spectra. Nonlinear response history analysis (NRHA) is carried out with the 2D models in both directions. At the BSE-2E level, 29 and 13 seismic records lead to collapse in X-and Y-loading directions, respectively. The collapses are mainly observed at the upper and lower levels in X- and Y-loading directions, respectively. Almost all beams exhibit yielding while panel zones remain elastic. Due to lack of capacity design requirements, the columns are subjected to excessive axial loads. This is more notable in end (i.e., exterior) columns of the X-direction frame. In this case, the compression forces reached up to the expected squash load in some records. Similarly, several of the

column splices particularly in end columns are found to be vulnerable. Further details regarding the design, modelling and seismic assessment of the tall building can be found in Akcelyan (2017).

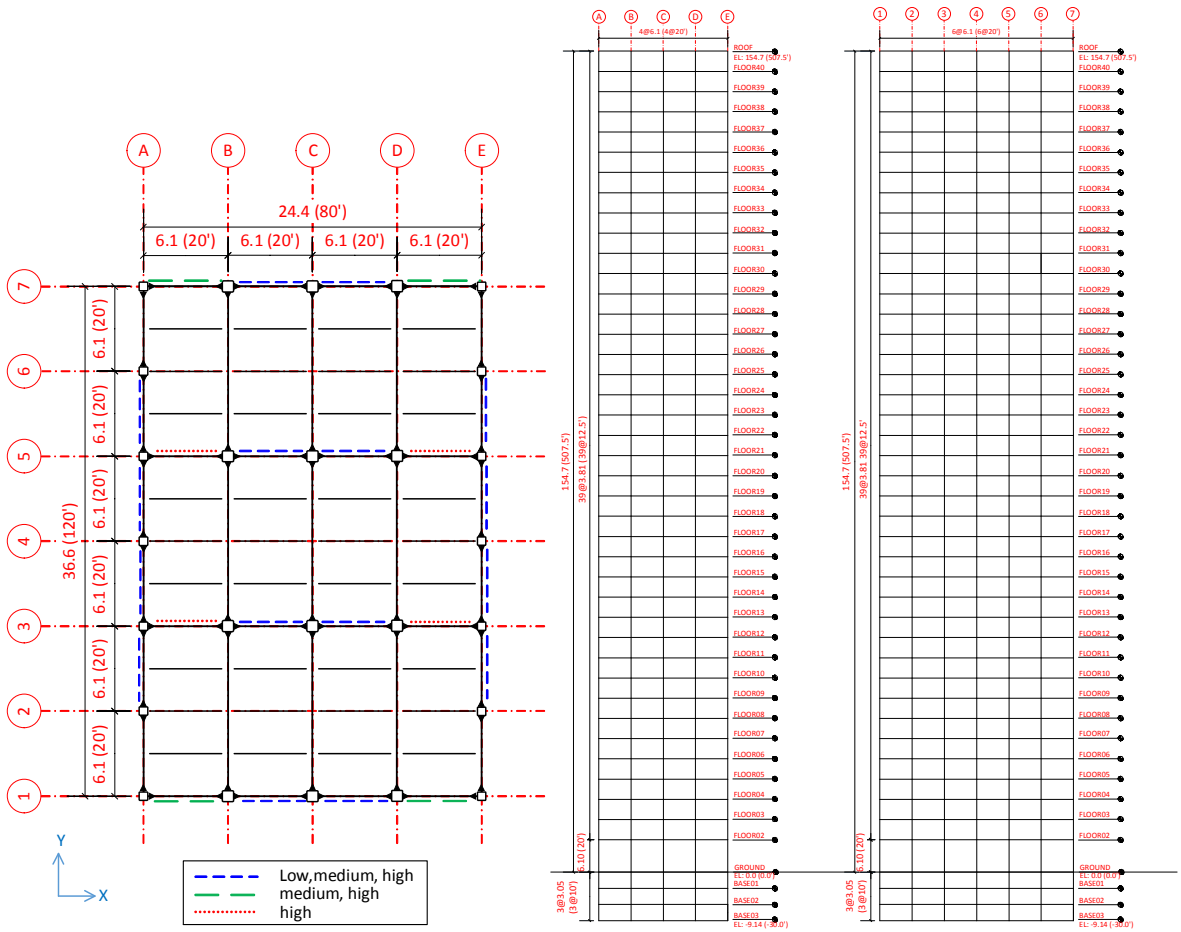

a) Floor plan b) X-loading direction c) Y-loading direction

Figure 1. Floor plan and elevation views of the building, dimensions in m (ft)

3. SEISMIC RETROFIT

3.1 Oil Damper with Relief Valve

Oil dampers contain low viscosity oil with a relief mechanism, which leads to a bilinear force-velocity relation. (F_d - $\acute{u}_d$) that can be expressed as follows (Ichihasi et al. 2000; Kasai and Nishimura 2004; Kasai et al. 2004; Tsuyuki et al. 2004; Yamamoto et al. 2016),

$$F_d(t)=\begin{cases} C_d\acute{u}_d(t), & |F_d(t)|\le F_{dr} \\ \mathrm{sgn}(\acute{u}_d(t))F_{dr}+p(\acute{u}_d(t)-\acute{u}_{dr}), & |F_d(t)|>F_{dr} \end{cases} \quad (1)$$

in which, C_d is the initial damping coefficient, p is the post relief damping coefficient ratio; F_{dr} and $\acute{u}_{dr}$ are the relief force and velocity of the bilinear oil damper, respectively. Under the assumption of sinusoidal displacement excitation $u_d(t) = u_{d0}\sin(\omega t)$, the peak damper force F_{d0} can be computed as follows,

$$F_{d0}=\left(p+\frac{1-p}{\mu_d}\right)C_d\omega u_{d0}, \quad \mu_d=\frac{\acute{u}_{d0}}{\acute{u}_{dr}}=\frac{\omega u_{d0}}{\acute{u}_{dr}} \quad (2)$$

in which, u_{d0} and ω are the peak displacement amplitude and the circular frequency of the sinusoidal excitation, respectively. μ_d is the peak damper velocity ratio, which is the ratio of maximum velocity demand over the damper relief velocity as given in Eq. 2. The force-displacement relation of a purely bilinear dashpot is illustrated in Figure 1a. In reality the damper assembly includes supporting brace stiffness (K_b) and internal damper stiffness (K_d), which can be represented as a Maxwell model with bilinear dashpot. This case is illustrated in Figure 2b. In order to solve the constitutive relation within the Maxwell model adaptive integration techniques were employed. The developed damper material model (noted as *BilinearOilDamper*) was implemented in the *OpenSees* platform (BilinearOilDamper 2015). Past research by the authors suggests that the damper stiffness should be considered because it typically reduces the damper efficiency significantly (Akcelyan et al. 2016). Figure 2c shows a single-degree-of-freedom (SDF) representation and the response of a shear building equipped with bilinear oil dampers. The loss stiffness (K_d'', K_a'', K'') and storage stiffness (K_a', K') of each system are highlighted in the same figures. The determination of the damper properties, such as the damper loss stiffness (K_d''), the brace stiffness (K_b) and their ratios to the frame stiffness (K_d''/K_{fs} and K_b/K_{fs}) is a fundamental point for an effective seismic retrofit design.

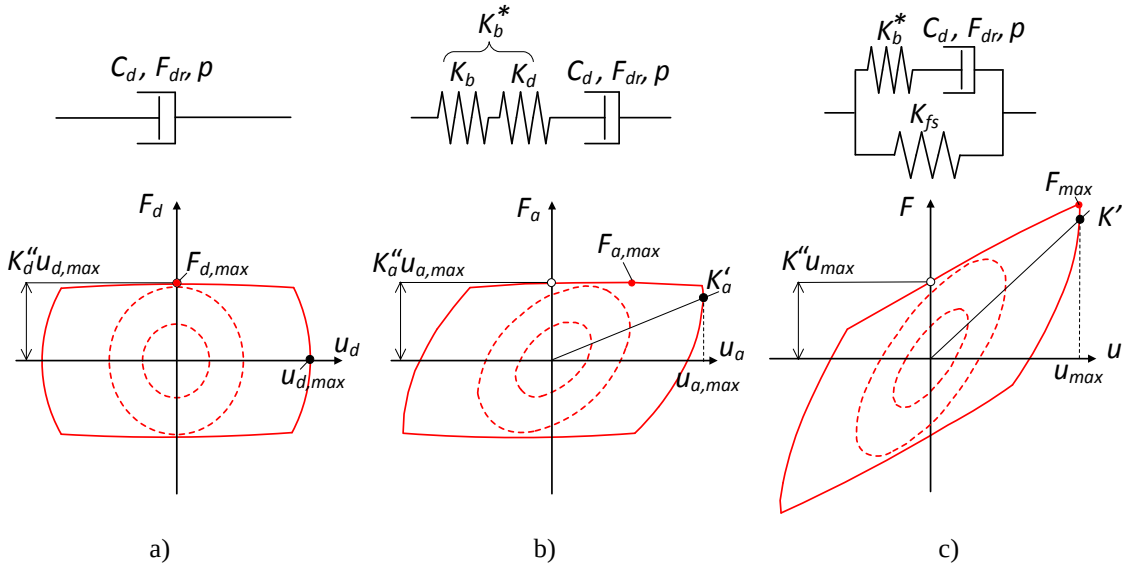

Figure 2. SDF representation of bilinear oil damper models and their force-displacement relations.

3.2 Design of Oil Dampers

Due to brevity, only the discussion focuses on the retrofit solution in the X-loading direction of the building. The oil damper design is carried out with the aid of MDF performance curves method (Akcelyan 2017). This tool utilizes performance curves (Kasai et al. 2008) as a preliminary design method and conducts intermediate evaluation via response history analysis of simplified MDF flexural shear beam models of the building equipped with dampers. Thus, by utilizing the MDF performance curves, the story-based engineering demand parameters (EDPs) can directly be obtained for a range of design solutions.

Nonlinear static analysis suggests that the global yielding of the building initiates at 0.5% roof drift. Therefore, keeping the frame entirely elastic requires almost a 70% displacement reduction (R_d = 0.3) with respect to the elastic response of the unretrofitted building. Based on the MDF performance curves such reduction is not feasible even for very large supplemental damping levels (K_d''/K_{fs} = 5). In addition, MDF performance curves indicate that the reductions in base shear and floor acceleration ceases for K_d''/K_{fs} > 1. Three levels of damping are considered reasonable to explore herein. These are named as low, medium and high damping levels, which have K_d''/K_{fs} =0.25, 0.5 and 1, respectively.

The seismic retrofit is conducted by using available damper sizes produced by an oil damper manufacturer. Maximum allowable damper forces of these dampers range from 250KN to 2000KN. Given the long fundamental period of the building, the damper sizes are selected with the lowest relief velocity (1.8 m/s) in order to maximize the peak damper velocity ratio (μ_d) and enable bilinear response of the oil dampers at the fundamental period of vibration of the benchmark building. These dampers have a post-relief damping coefficient ratio of p = 0.017. Typically, the K_b / K_{fs} becomes the highest at the highest damping level (K_d'' / K_{fs}). Therefore, it is more reasonable to compare the ratio of the damper brace stiffness to the damper loss stiffness (K_b / K_d''), which is relatively constant. In the evaluated retrofit schemes, the overall K_b / K_d'' ratio is between 4.4 and 6.3 while the overall K_b^* / K_d'' ratio ranges from 1.6 to 2.4. Thus, it can be conservatively assumed that K_b / K_d'' = 4.0 for the initial equivalent SDF design. Based on the performance curves method, the effective damping ratios are estimated to be 7, 13 and 22%, for low, medium and high damping levels, respectively. The corresponding displacement reduction factors (R_d) are 0.64, 0.48 and 0.36, respectively.

3.3 Horizontal Distribution of Supplemental Damping

Dampers are installed as diagonal braces mainly in exterior frames (see Figure 1a) because this configuration is more effective for controlling torsional vibrations. A comparative study was conducted regarding the horizontal placement of dampers by analyzing two retrofit schemes, in which dampers were installed in interior and exterior bays of the exterior frames, respectively. The outcome indicates that dampers are more efficient if they are installed in interior bays. This is attributed to the high axial deformation of end columns, which causes flexural deformations; hence, a reduction in damper efficiency is implied. Placing dampers in exterior bays may considerably increase the already high column axial force demands. Therefore, dampers are also installed in interior bays of interior frames in the X-loading direction, particularly in case of medium and high damping levels.

3.4 Vertical Distribution Methods for Supplemental Damping

Three story shear force proportional damping distribution (SFPDD) methods are considered herein namely direct, effective and proposed balanced SFPDD methods. The three retrofit schemes for medium damping level are illustrated in Figure 3 for the aforementioned methods. In these figures, the damper locations are indicated with their corresponding maximum damper forces (in KN). If dampers are designed based on the direct SFPDD method, their storage stiffness (K_a') at each story is determined directly proportional to the story shear force (see Figure 3a). In this method dampers are provided at all levels, however, the impact of the building's story stiffness distribution on the damping distribution is ignored. Alternatively, the effective storage force (K') at each story is determined proportionally to the story shear force when the effective SFPDD method is employed. As the effective storage stiffness is composed of frame stiffness (K_{fs}) and damper storage stiffness (K_a') (see Figure 2c), dampers are mainly placed at stories where supplemental effective storage stiffness is required as shown in Figure 3b. Thus, effective SFPDD aims to achieve a uniform drift distribution for a given story shear force distribution along the building height (Kasai et al. 2008). A fair comparison can be done if for all the distribution methods care is given to keep the overall damping properties constant at each damping level and not to oversize dampers.

The comparative study with nine retrofit schemes is employed in the X-loading direction by utilizing ten ground motions, which led to collapse of the original building at BSE-2E level. Figure 4 illustrates median peak SDRs obtained from low (L), medium (M) and high (H) damping levels, respectively for the implementation of effective (E), direct (V) and balanced (B) SFPDD methods. The effective SFPDD leads to high peak SDR concentration in the bottom stories for low and medium damping levels. This is attributed to the fact that no dampers were placed at lower stories according to the effective SFPDD method. As a result, 4 and 3 collapses were observed at low and medium damping levels, respectively. In contrast, peak SDRs take place in the upper stories if the direct SFPDD method is employed. Only one collapse is observed in this case at the low damping level. While the damping level increases, differences in peak SDRs become less distinct. This is attributed to the limited frame inelastic action. Notably, collapse is prevented in this case.

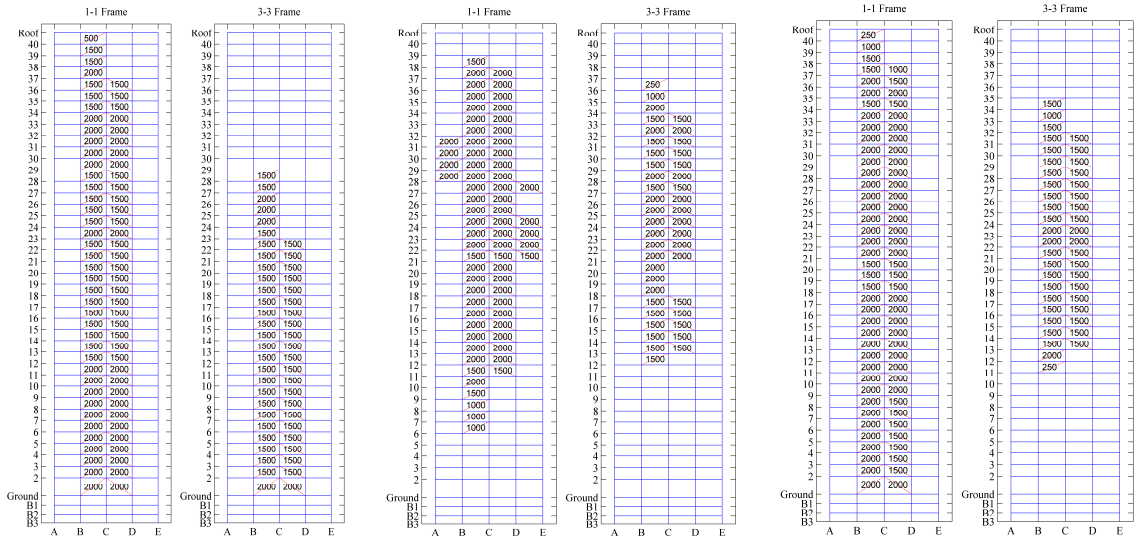

Figure 3. Damper design (maximum allowable forces in KN), medium damping level X-loading direction

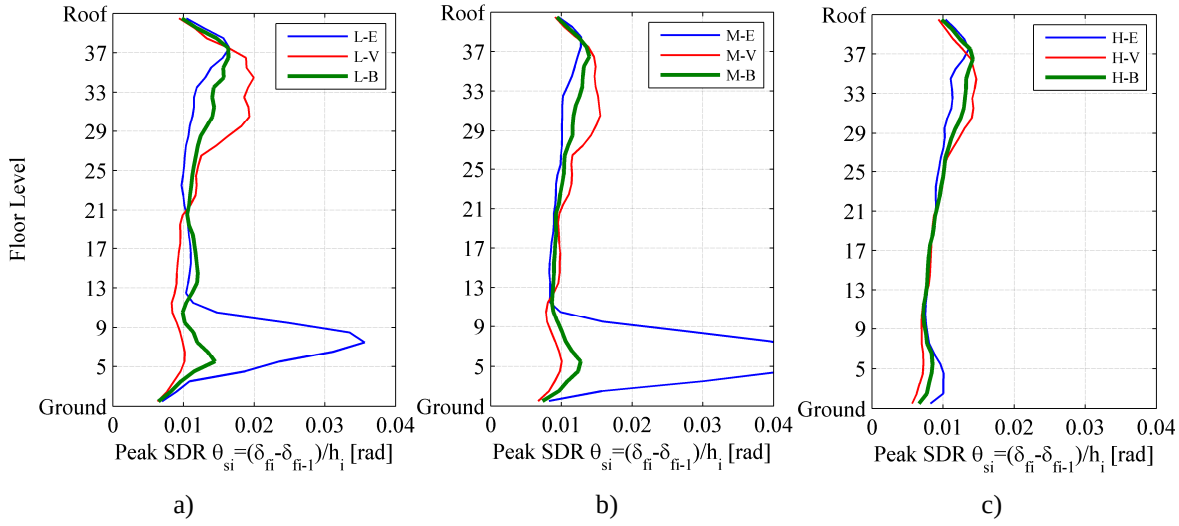

Figure 4. Peak story drift ratios of nine retrofit schemes

3.5 Balanced Distribution

Conventional damping distribution methods are based on elastic properties of the building to be retrofitted. Despite of the retrofit, structural damage is almost inevitable under a low probability of occurrence earthquake. For instance, the effective SFPDD method led to the most inefficient retrofit solution at low and medium damping levels, because the frame was not able to maintain its elastic stiffness at large story drifts. The direct SFPDD method provided a more redundant damper distribution along the building height. This is because it follows directly the story shear force distribution. However, the stiffness distribution of the frame to be retrofitted is ignored in this case. This may result into inefficient retrofit solutions particularly if the building possesses high irregularities in story stiffness along the height and/or if story drifts are relatively low. An alternative SFPDD method, balanced distribution was proposed to circumvent the aforementioned challenges that combines the two preceding methods. Thus, according to the balanced SFPDD method the loss stiffness of dampers at each story $K''_{di,B}$ can be computed as follows,

$$K''_{di,B} = \gamma K''_{di,E} + (1-\gamma) K''_{di,V} \quad (3)$$

In which $K''_{di,E}$ and $K''_{di,V}$ are the loss stiffness of dampers computed based on effective and direct SFPDD, respectively; γ is a weight factor, ranging between 0 and 1. If $\gamma = 0$, the damping distribution becomes identical with the direct SFPDD, hence, the effect of frame elastic stiffness is neglected and dampers are placed at all levels. If $\gamma = 1$, the effect of elastic frame stiffness is fully considered, as in the case of effective SFPDD, dampers may be placed at fewer stories. Between these two extreme cases ($0 < \gamma < 1$) elastic frame stiffness is partially considered and dampers are placed at all levels. Thus, the balanced SFPDD method accounts for the vertical frame stiffness distribution. In the retrofit under consideration, frame yielding is expected; therefore, only a fraction of the elastic frame stiffness is expected to be effective; thus, the balanced SFPDD method is utilized by assuming $\gamma = 0.5$.

Referring to Figure 4, the median peak SDRs obtained from the balanced distribution method are superimposed. It is shown that the balanced distribution method provides the most uniform peak SDR distribution along the building height. For instance, at the medium damping level the peak SDRs are below 1.5% in 5 cases, compared to 3 and 2 cases observed in the effective and direct SFPDD methods, respectively. At a low damping level, the balanced SFPDD leads to 2 bottom story collapses, compared to 4 and 1 observed in the effective and direct SFPDD methods, respectively. This implies that a uniform distribution of peak SDRs does not always guarantee the least damage/number of collapses. In tall MRF buildings it is common to have large flexural deformation in the upper stories. This is due to the column axial elongation/shortening. Therefore, for a uniform SDR distribution, shear demands are larger at lower stories to balance the flexural deformation in the upper stories. This typically leads to damage concentration in the lower stories.

Figure 5 shows the histogram of peak SDRs in the X-direction obtained from NRHA of 40 GMs at the BSE-2E seismic intensity for low, medium and high damping levels designed based on a balanced distribution. The outcome of the unretrofitted building is superimposed for comparison purposes. The number of collapses reduced from 29 to 10 and 4 at low and medium damping levels, respectively. No collapses occurred at a high damping level. The peak SDRs range between 0.01-0.02 rad as the damping level increases.

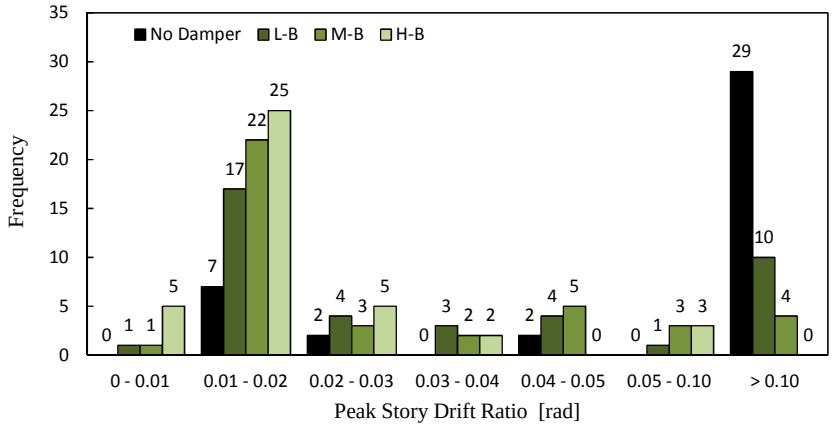

Figure 5. Peak SDRs with different damping level using the balanced SFPDD method (BSE-2E level)

3.6 Final Retrofit Solution

The final retrofit design is selected based on the balanced distribution method considering its efficient SDR control along the building height. Medium damping level is chosen because the collapse prevention objective is achieved. Figures 6 and 7 illustrate the peak story-based EDPs of the retrofitted building obtained from NRHAs of 40 records that are scaled at BSE-1E and BSE-2E seismic intensities, respectively. The median, 16th and 84th percentile responses are also shown in the same figures. From the unretrofitted building assessment, upper story collapses were observed due to drift concentrations. Referring to median response in Figures 6 and 7, the peak SDR profile becomes

relatively uniform at both seismic levels due to the efficiency of the proposed retrofit solution. At higher seismic intensities, the damage concentrates mainly in the lower stories (see Figure 7a). The median peak absolute floor accelerations range between 0.4 and 0.6g at BSE-1E and BSE-2E seismic intensities, respectively.

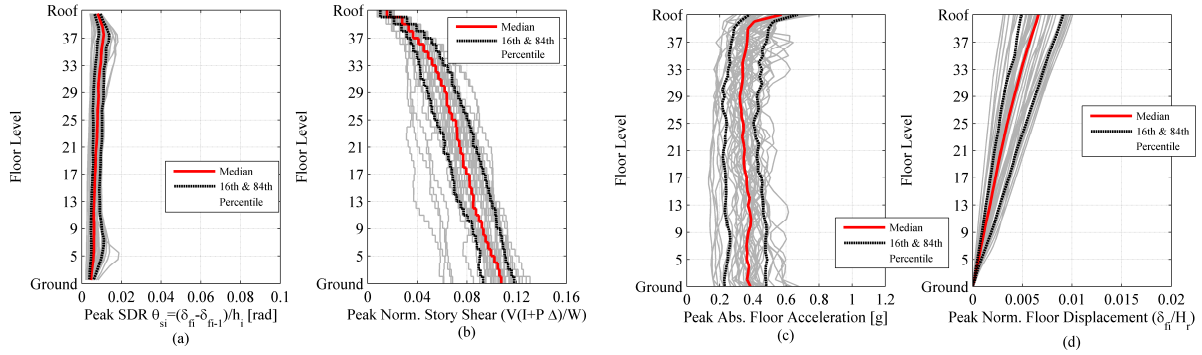

Figure 6. Engineering demand parameters of the retrofitted building (BSE-1E)

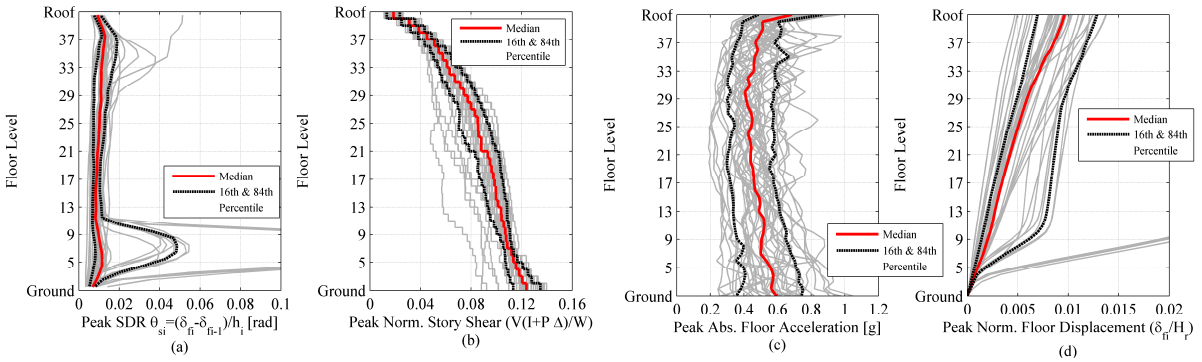

Figure 7. Engineering demand parameters of the retrofitted building (BSE-2E)

Figure 8a is the histogram of the peak SDR of the original (ND) and retrofitted building (M-B) at BSE-1E and BSE-2E seismic intensities. The histogram of residual SDRs is plotted in Figure 8b. No collapse was observed at BSE-1E level and in 32 records the residuals SDR didn't exceed 0.2%. This indicates that the building practically remains elastic for most of the records scaled at the BSE-1E intensity. Unlike the unretrofitted building, residual deformations are mainly observed in the bottom stories of the building.

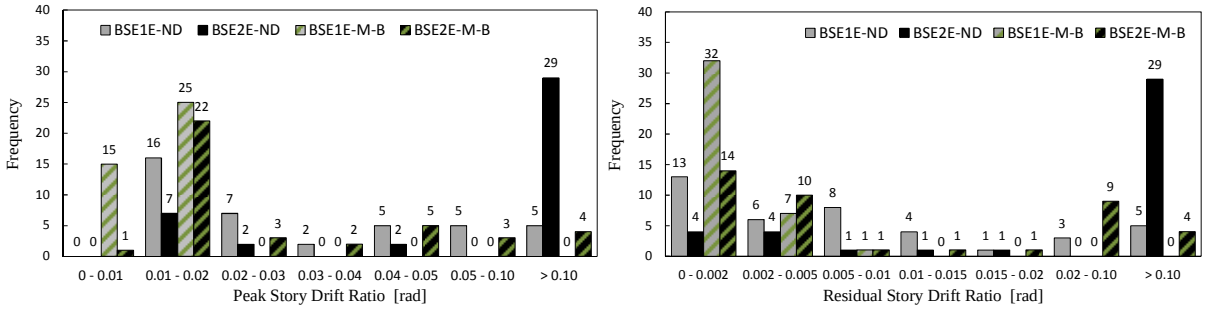

a) b)

Figure 8. Peak and residual SDRs of the retrofitted building

Other aspects to be considered include the peak damper demands, such as the damper stroke, the velocity and force for the final verification of damper properties. For instance, the median peak

damper strokes are found to be less than 30mm at the BSE-2E seismic intensity. This is well below the smallest stroke capacity of the oil dampers (60mm). At the same intensity level, the median values of peak post-relief velocity ratios are between 2.3 and 9.8. Larger values are observed in the top and bottom stories, while for the dampers at mid-stories the same ratio is around 3. Figure 8 shows oil damper force displacement relations obtained from one ground motion record (Westmorland Fire Station-360, 2010 El Mayor Cucapah Mexico Earthquake) that is scaled at the BSE-2E seismic intensity. Referring to Figure 8c, dampers in 40th story exhibit high velocity demands; however, forces remain relatively constant and below the 250KN damper force capacity. The relief mechanism is activated at this force level. Referring to Figure 8c, the force-displacement relation in this case resembles a friction damper. On the other hand, the force-displacement relation of the 20th story damper (1500KN capacity) is relative round and less nonlinear due to lower velocity demands observed in the mid-stories of the building. This underscores another advantage of bilinear oil dampers that at low and moderate ground shaking intensities large amount of supplemental damping can be provided with their initial linear viscous characteristics.

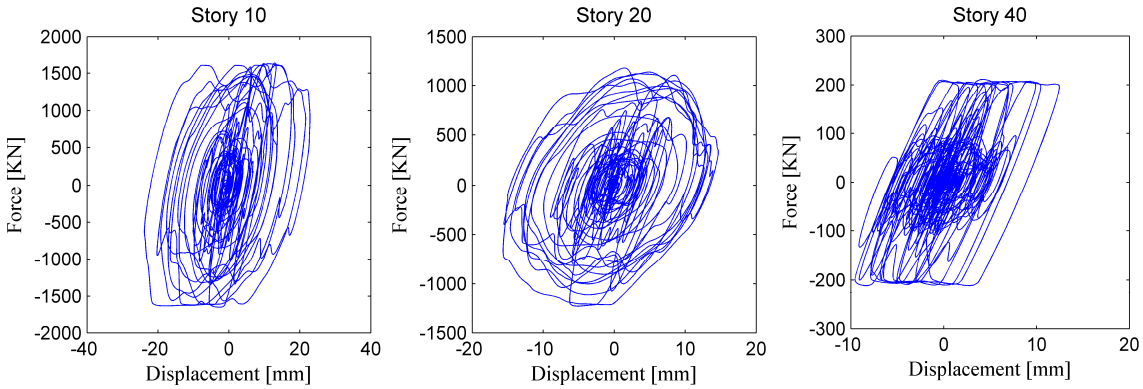

Figure 8. Damper force-displacement relation for one ground motion record (Westmorland Fire Station-360, 2010 El Mayor Cucapah Mexico Earthquake, scaled at BSE-2E)

As the dampers mitigate collapses in the upper stories, there is no evidence of inelastic behavior in upper story columns and their splices, based on the 84th percentile at the BSE-2E seismic intensity. Although the dampers did not result into significant increase in column axial loads, the EDP reduction did not improve the situation for end columns in lower stories of the building. Same observations hold true for column splices.

4. CONCLUSIONS

This paper presented multiple seismic retrofit strategies for a benchmark pre-Northridge steel tall building by utilizing supplement damping via bilinear oil dampers. To this end, nine retrofit schemes were designed with three different damping levels (K_d'' / K_{fs} =0.25, 0.5 and 1) and distribution methods. In these retrofit options the K_b / K_d'' ratio was between 4.4 and 6.3 while K_b^* / K_d'' ratio varied between 1.6 to 2.4. It was found that the level of frame inelasticity had a strong impact on the efficiency of damping distributions methods. If collapse prevention is the main performance objective, then the direct SFPDD method provided the most efficient retrofit solution. In this case, the peak SDRs were larger in the upper stories.

A balanced SFPDD was proposed as a hybrid distribution of effective and direct SFPDD methods. This distribution aims to be more redundant for collapse prevention than effective SFPDD. At the same time, unlike direct SFPDD, it accounts for possible vertical irregularities in the frame stiffness. Thus, the proposed balanced SFPDD provided an efficient retrofit solution, particularly at a medium damping level. Collapses observed at upper stories were eliminated. The number of collapses reduced from 29 to 4 at the BSE-2E level, while no collapse was observed at the BSE-1E level. For most of the

examined records, the residual SDRs along the height of the building were below 0.2% at the same seismic intensity.
Damper velocity demands were higher in the mid- to upper stories; however, the damper forces remained relatively constant. This eliminates the uncertainties in the expected damper forces and allows for a less conservative non-dissipative member design. Furthermore, dampers dissipated significant amount of energy at lower shaking intensities. Both the column and the splice demands were reduced in the upper stories, while the end column seismic demands were still fairly large.

5. ACKNOWLEDGMENTS

The authors would like to acknowledge the financial support from Fonds de recherche du Québec Nature et technologies (FQRNT) and the Natural Sciences and Engineering Research Council of Canada (NSERC) for the doctoral studies of the first author at McGill University. The findings in this paper are those of the authors and do not necessary reflect the view of the sponsors.

6. REFERENCES

Akcelyan, S. (2017). Seismic retrofit of existing steel tall buildings with supplemental damping devices. *Ph.D. Dissertation*, McGill University.

Akcelyan, S., Lignos, D. G., Hikino, T., and Nakashima, M. (2016). Evaluation of simplified and state-of-the-art analysis procedures for steel frame buildings equipped with supplemental damping devices based on E-Defense full-scale shake table tests. *Journal of Structural Engineering*, 142(6), 04016024.

Almufti, I., Hutt, C. M., Willford, M., and Deierlein, G. (2012). Seismic assessment of typical 1970s tall steel moments frame buildings in downtown San Francisco. *Proc., 15th World Conference of Earthquake Engineering*, Lisbon, Portugal.

ASCE/SEI (2014). Seismic evaluation and retrofit of existing buildings. *ASCE/SEI 41-13*, American Society of Civil Engineers, Reston, VA.

Bech, D., Tremayne, B., and Houston, J. (2015). Proposed changes to steel column evaluation criteria for existing buildings. *Proc. Improving the Seismic Performance of Existing Buildings and Other Structures 2015*, 255-272.

BilinearOilDamper (2015). BilinearOilDamper material. *OpenSeesWiki online manual*, <http://opensees.berkeley.edu/wiki/index.php/BilinearOilDamper_Material>. (Aug. 6, 2015).

Constantinou, M., Symans, M., Tsopelas, P., and Taylor, D. (1993). Fluid viscous dampers in applications of seismic energy dissipation and seismic isolation. *Proc., ATC 17-1 Seminar on Seismic Isolation, Passive Energy Dissipation, and Active Control*, 2, 581-592.

Galasso, C., Stillmaker, K., Eltit, C., and Kanvinde, A. (2015). Probabilistic demand and fragility assessment of welded column splices in steel moment frames. *Earthquake Engineering & Structural Dynamics*, 44(11), 1823-1840.

Hutt, C. M., Almufti, I., Willford, M., and Deierlein, G. (2016). Seismic loss and downtime assessment of existing tall steel-framed buildings and strategies for increased resilience. *Journal of Structural Engineering*, 142(8), C4015005.

Ibarra, L. F., and Krawinkler, H. (2005). Global collapse of frame structures under seismic excitations, Pacific Earthquake Engineering Research Center.

ICBO (1973). Uniform Building Code (UBC). International Conference of Building Officials, Washington, DC.

Ichihasi, S., Okuzono, T., Takahashi, O., Usami, M., Ninomiya, M., Tsuyuki, Y., and Ishida, Y. (2000). Vibration test of a frame which has an oil-damper brace. *Proc., The 12th World Conference on Earthquake Engineering (WCEE)*, Auckland, New Zealand.

Kasai, K., Ito, H., and Ogura, T. (2008). Passive control design method based on tuning of equivalent stiffness of bilinear oil dampers. *Journal of structural and construction engineering*, 73(630), 1281-1288.

Kasai, K., Lu, X., Pu, W., Yamashita, T., Arakawa, Y., and Zhou, Y. (2013). Effective retrofit using dampers for a steel tall building shaken by 2011 East Japan Earthquake: China-Japan cooperation program (Part 2). *Proc., 10th International Conference on Urban Earthquake Engineering (10CUEE)*, Tokyo Institute of Technology,

Tokyo, Japan.

Kasai, K., and Matsuda, K. (2014). Full-scale dynamic testing of response-controlled buildings and their components: concepts, methods, and findings. *Earthq. Engin. Engin. Vib.*, 13(1), 167-181 English.

Kasai, K., Mita, A., Kitamura, H., Matsuda, K., Morgan, T. A., and Taylor, A. W. (2013b). Performance of seismic protection technologies during the 2011 Tohoku-Oki Earthquake. *Earthquake Spectra*, 29(S1), S265-S293.

Kasai, K., and Nishimura, T. (2004). Equivalent linearization of passive control system with oil damper bilinearly dependent on velocity. *Journal of Structural and Construction Engineering, AIJ*, (583), 47-54 (in Japanese).

Kasai, K., Takahashi, O., and Sekiguchi, Y. (2004). JSSI manual for building passive control technology part-10 time-history analysis model for nonlinear oil dampers. *Proc., The 13th World Conference on Earthquake Engineering*, Vancouver, B.C., Canada.

Krawinkler, H. (1978). Shear in beam-column joints in seismic design of steel frames. *Engineering Journal*, 15(3), 82-91.

Lai, J.-W., Schoettler, M., Wang, S., and Mahin, S. (2015). Seismic evaluation and retrofit of existing tall buildings in California: Case study of a 35-story steel moment resisting frame building in San Francisco. *PEER 2015/14*, Pacific Earthquake Engineering Research Center Headquarters at the University of California, Berkeley.

Lignos, D. G., Hartloper, A., Elkady, A., Hamburger, R., and Deierlein, G. G. (2018). Revised ASCE-41 modeling recommendations for moment-resisting frame systems. *Proc., 11th National Conference in Earthquake Engineering*, Earthquake Engineering Research Institute, Los Angeles, CA.

Lignos, D. G., and Krawinkler, H. (2011). Deterioration modeling of steel components in support of collapse prediction of steel moment frames under earthquake loading. *Journal of Structural Engineering*, 137(11), 1291-1302.

Malley, J. O., Sinclair, M., Graf, T., Blaney, C., and Ahmed, T. (2011). Incorporation of full-scale testing and nonlinear connection analyses into the seismic upgrade of a 15-story steel moment frame building. *The Structural Design of Tall and Special Buildings*, 20(4), 472-481.

McKenna, F. T. (1997). Object-oriented finite element programming: frameworks for analysis, algorithms and parallel computing. *Ph.D. Dissertation*, University of California, Berkeley.

Stillmaker, K., Kanvinde, A., and Galasso, C. (2016). Fracture mechanics-based design of column splices with partial joint penetration welds. *Journal of Structural Engineering*, 142(2), 04015115.

Symans, M., Charney, F., Whittaker, A., Constantinou, M., Kircher, C., Johnson, M., and McNamara, R. (2008). Energy dissipation systems for seismic applications: current practice and recent developments. *Journal of Structural Engineering*, 134(1), 3-21.

Symans, M. D., and Constantinou, M. C. (1998). Passive fluid viscous damping systems for seismic energy dissipation. *ISET Journal of Earthquake Technology*, 35(4), 185-206.

Tsuyuki, Y., Gofuku, Y., Iiyama, F., and Kotake, Y. (2004). JSSI manual for building passive control technology part-3 performance and quality control of oil damper. *Proc., The 13th World Conference on Earthquake Engineering*, Vancouver, B.C., Canada.

Uriz, P., and Whittaker, A. S. (2001). Retrofit of pre-Northridge steel moment-resisting frames using fluid viscous dampers. *The Structural Design of Tall Buildings*, 10(5), 371-390.

Yamamoto, M., Minewaki, S., Nakahara, M., and Tsuyuki, Y. (2016). Concept and performance testing of a high-capacity oil damper comprising multiple damper units. *Earthquake Engineering & Structural Dynamics*, 45(12), 1919-1933.

Zareian, F., and Krawinkler, H. (2006). Simplified performance-based earthquake engineering. Stanford University Stanford, CA, USA.